

STAMP2 Attenuates Cardiac Dysfunction and Insulin Resistance in Diabetic Cardiomyopathy via NMRAL1-Mediated NF- κ B Inhibition in Type 2 Diabetic Rats

Zhan Gao^{1,2}, Yun Ti¹, Bin Lu¹, Fang-qiang Song^{1,3}, Lei Zhang¹, Bo-ang Hu¹, Jia-ying Xie¹, Wei Zhang¹, Lu Han^{1,4}, Ming Zhong¹

¹The Key Laboratory of Cardiovascular Remodeling and Function Research, Chinese Ministry of Education, Chinese National Health Commission and Chinese Academy of Medical Sciences, The State and Shandong Province Joint Key Laboratory of Translational Cardiovascular Medicine, Department of Cardiology, Qilu Hospital, Qilu College of Medicine, Shandong University, Jinan, People's Republic of China; ²Department of Cardiology, The First Affiliated Hospital of Wenzhou Medical University, Wenzhou, People's Republic of China; ³Department of Critical Care Medicine, Tengzhou Central People's Hospital, Tengzhou, People's Republic of China; ⁴Department of General Practice, Qilu Hospital, Qilu College of Medicine, Shandong University, Jinan, People's Republic of China

Correspondence: Lu Han; Ming Zhong, Email luhan_sdu@163.com; zhongming2sdu@163.com

Background: Previous studies have reported that six transmembrane protein of prostate 2 (STAMP2) attenuates metabolic inflammation and insulin resistance in diabetes mellitus. However, the role of STAMP2 in the diabetic heart is still unclear.

Methods: A diabetic rat cardiomyopathy model was established via intraperitoneal STZ injection. STAMP2 was overexpressed in the treatment group using adeno-associated virus. Rat heart diastolic function was measured using echocardiography and a left ventricular catheter, and cardiac interstitial fibrosis was detected by immunohistochemistry and histological staining. Insulin sensitivity and NF- κ B expression were shown by Western blotting. NMRAL1 distribution was illustrated by immunofluorescence.

Results: STAMP2 expression in the diabetic rat heart was reduced, and exogenous overexpression of STAMP2 improved glucose tolerance and insulin sensitivity and alleviated diastolic dysfunction and myocardial fibrosis. Furthermore, we found that NF- κ B signaling is activated in the diabetic heart and that exogenous overexpression of STAMP2 promotes NMRAL1 translocation from the cytoplasm to the nucleus and inhibits p65 phosphorylation.

Conclusion: STAMP2 attenuates cardiac dysfunction and insulin resistance in diabetic cardiomyopathy, likely by promoting NMRAL1 retranslocation and NF- κ B signaling inhibition.

Keywords: STAMP2, diabetic cardiomyopathy, NADPH, NMRAL1, NF- κ B

Introduction

Diabetes mellitus has caused tremendous health and economic burdens worldwide. Among them, heart failure and other cardiovascular complications have been demonstrated to be the most common cause of death. Diabetic cardiomyopathy (DCM) greatly increases the incidence and mortality of heart failure.¹ DCM is characterized by overt myocardial interstitial fibrosis and decreased diastolic function. Numerous theories have been proposed to explain the mechanism of severe interstitial fibrosis. Insulin resistance is indicated by abundant research to trigger DCM occurrence and development.² However, the mechanism underlying insulin resistance and leading to altered myocardial structure remains incompletely understood.

STAMP2 (six-transmembrane protein of prostate 2), also known as STEAP4 (six-transmembrane epithelial antigen of prostate 4), belongs to a family of six-transmembrane proteins. Three of the four family members, including STAMP2, have been characterized as reductases because they all have NADPH oxidoreductase motifs.³ Recent studies have found that STAMP2 significantly improves insulin resistance in a variety of cells and animal models. For example, STAMP2 knockout

mice exhibit overt inflammation, spontaneous insulin resistance, glucose intolerance, mild hyperglycemia, dyslipidemia, and fatty liver disease,⁴ while overexpressing STAMP2 in diabetic mice reduced proinflammatory cytokine levels and improved insulin resistance by inhibiting JNK phosphorylation.⁵ Accelerated hepatic steatosis and insulin resistance were observed in STAMP2 knockout mice; conversely, adenoviral STAMP2 improved hepatocyte lipid accumulation, hepatic steatosis and insulin resistance via sterol response element binding protein 1 (SREBP1) and the PPAR γ pathway.⁶ To date, two questions remain unanswered. First, how is STAMP2 capable of alleviating metabolic disorders, inflammatory signaling and insulin resistance? Additionally, although DCM is a typical metabolic disease and the heart is an organ with high STAMP2 expression,⁷ there has not been any research concerning STAMP2 in DCM.

We assume that the biological function of STAMP2 is mediated by its NADPH oxidoreductase motif. NADPH can transmit cellular signals in multiple ways. Previous research has found that intracellular NADPH can be sensed by the NADPH sensor protein NMRAL1 (nmra-like family domain-containing protein 1). When NADPH is decreased, NMRAL1 migrates from the cytoplasm to the nucleus and inhibits p65 phosphorylation.^{8,9} There is abundant evidence linking NF- κ B activation to myocardial insulin resistance.¹⁰

Therefore, we hypothesized that heart STAMP2 plays a protective role in DCM that depends on its NADPH oxidoreductase motif and the cellular NADPH sensor protein NMRAL1. As will be shown, we established a DCM model in type 2 diabetic rats and confirmed insulin resistance in model rats by examining Akt signaling, overt cardiac fibrosis using immunohistochemistry, and cardiac diastolic dysfunction via echocardiography and left ventricular catheterization. Then, STAMP2 was exogenously introduced into diabetic rat hearts via adeno-associated virus. Our data indicate that STAMP2 is decreased in DCM and that overexpression of STAMP2 improves cardiac fibrosis, diastolic dysfunction and insulin resistance in type 2 diabetic hearts via NMRAL1-mediated NF- κ B inhibition.

Materials and Methods

Animals and Treatment

Four-week-old male Sprague–Dawley rats weighing 100–120 g were randomized into a control group and type 2 diabetes mellitus (DM) group. Rats in the control group were fed a regular diet. Rats in the type 2 diabetes mellitus group were fed a high-fat diet (34.5% fat, 17.5% protein, 48% carbohydrate; Beijing HFK Biotechnology, China), and type 2 diabetes mellitus was induced at the age of 9 weeks by a single intraperitoneal injection of streptozotocin (STZ, Sigma–Aldrich, St. Louis, MO, USA) at a dose of 27.5 mg/kg dissolved in 100 mm citrate buffer (pH 4.5). DM was diagnosed by two continuous fasting blood glucose tests one week after STZ intraperitoneal injection. Rats with a blood sugar level higher than 11.1 mmol/L were enrolled in further study. At the age of 22 weeks, rats with similar blood sugar values and weights were randomly divided into 3 groups: the STAMP2 group containing type 2 diabetic rats receiving recombinant STAMP2-expressing serotype 9 adeno-associated virus (AAV9) via intrajugular vein injection (Hanbio Biotechnology, China); the vehicle group containing type 2 diabetic rats receiving blank AAV9 vector; and the DM group containing type 2 diabetic rats not receiving AAV9. Four weeks after transfection, ie, at the age of 26 weeks, rats were sacrificed, and hearts were collected for further study. For each experiment, 6–8 rats were used to calculate the result. All animal procedures in the present study were performed under the supervision of the Institutional Animal Care and Use Committee of Shandong University in accordance with the Regulations for the Laboratory Animals issued by the National Science and Technology Commission.

Glucose Tolerance Test, Insulin Tolerance Test and Serum Insulin

Intraperitoneal glucose tolerance tests (IPGTTs) and intraperitoneal insulin tolerance tests (IPITTs) were performed at 4 w, 9 w, 22 w and 26 w. Before examination, blood samples for determination of the fasting serum insulin level were taken after the rats were fasted overnight. Then, 1 g/kg glucose or 1 U/kg insulin (Regular Humulin, Eli Lilly and Company) was injected intraperitoneally, and blood glucose was recorded at 0, 15, 30, 60 and 120 min following intraperitoneal injection using One-Touch Ultra glucometers. The mean area under the curve (AUC) was calculated. The insulin sensitivity index (ISI) was calculated according to serum insulin and blood glucose levels $ISI = \ln(\text{serum insulin} \times \text{blood glucose})^{-1}$.

Echocardiography and Left Ventricular Catheterization

Echocardiography was performed at 4 w, 16 w, 22 w and 26 w for each rat using a Vevo770 animal echocardiography machine (Visual Sonics Inc.). Systolic and diastolic left ventricular posterior wall thickness, septum thickness, left ventricular diameter, left ventricular ejection fraction (LVEF) and fractional shortening (FS) were measured from the parasternal long-axis view via two-dimensional and M-mode ultrasound. Transmitral flow velocity variables, including peak E, peak A, and the E-to-A (E/A) ratio, were measured from the apical four-chamber view via mitral-valve pulsed Doppler. Tissue Doppler imaging of the mitral annulus was used to analyze early (E'), late (A') diastolic velocity and the E'/A' and E/E' ratios.

Hemodynamic measurements were recorded through left ventricular catheterization via the right carotid artery at 26 w, immediately before the rats were sacrificed. Data, including left ventricular end-diastolic pressure (LVEDP) and dp/dt, were collected and analyzed using the Powerlab system coupled to Labchart software (ADInstruments, California).

Histologic, Immunohistochemical and Immunofluorescence Staining

For histopathological analyses, mid-ventricular sections of the left ventricle were excised, fixed (4% paraformaldehyde), dehydrated, and embedded in paraffin. Four-micrometer-thick sections were prepared for further studies. Hematoxylin-eosin staining was used to show general ventricular wall morphology changes. Fluorescein isothiocyanate-conjugated wheat germ agglutinin (WGA; Invitrogen) was adopted for membrane staining to show the cross-sectional cardiomyocyte area. Masson staining was used to indicate collagen deposition. Sections were also incubated with primary antibodies against collagen I (Proteintech, China) and collagen III (Proteintech, China) to measure type I and III collagen deposition. For immunofluorescence (IF), sections were incubated with anti-NMRAL1 antibody (Proteintech, China) after protein blocking, antigen retrieval, and permeabilization. Subsequently, sections were stained with secondary antibody (conjugated with Alexa Fluor[®] 488) and DAPI. Slides were photographed with a Panoramic MIDI-II Digital Scanner (3DHISTECH, Budapest, Hungary), and the results were analyzed using ImageJ with the IHC Profiler plugin and the Coloc 2 plugin.

Western Blotting

Total protein samples were extracted from the left ventricular lysates and subsequently separated via SDS-PAGE. STAMP2 was detected with a polyclonal antibody (Proteintech, China), and antibodies against Akt (CST, USA), phospho-Akt (p-Akt) (Ser473) (CST, USA), and insulin receptor substrate-1 (IRS-1) (CST, USA) were applied to investigate Akt signaling and insulin resistance. Antibodies against NF- κ B p65 (CST, USA) and phospho-NF- κ B p65 (p-p65) (Ser536) (CST, USA) were used to investigate NF- κ B activation. STAMP2 and IRS-1 protein levels were normalized to that of β -actin as an internal control. p-p65 and p-Akt levels were normalized to total p65 and Akt protein levels. The results were analyzed with ImageJ software.

Statistical Analysis

Statistical analysis was performed using SPSS 20.0 and GraphPad Prism 7.0 software. Data are shown as the means \pm standard deviations or standard error. Comparisons of IPGTT, IPITT, fasting serum insulin, and insulin resistance index results are shown as *t*-test result for the AUC of the glucose curve; comparisons of echocardiography, left ventricular catheterization parameters, immunohistochemistry and Western blotting results were performed using *t*-tests; comparisons of NMRAL1 intra- and extranuclear distribution were performed with χ^2 tests. *p* values under 0.05 were considered significant.

Results

Diabetic Rats Exhibited Overt Hyperglycemia, Insulin Resistance, Cardiac Diastolic Dysfunction and Fibrosis

GTTs and ITTs

Compared to the control group, the AUC of the blood glucose curve was significantly higher in diabetic rats for both the IPGTTs (3297.1 \pm 808.7 vs 1027.6 \pm 156.8, *p* <0.01, [Figure 1A](#)) and IPITTs (1315.7 \pm 234.9 vs 378.7 \pm 80.2, *p* <0.01, [Figure 1B](#)). Although fasting serum insulin was not significantly increased in diabetic rats ([Figure 1C](#)), the insulin resistance index was markedly decreased (-6.1 \pm 0.1 vs -4.7 \pm 0.1, *p*<0.01, [Figure 1D](#)).

Ultrasonic and hemodynamic findings

Diabetic rats exhibited distinct diastolic dysfunction after intraperitoneal streptozotocin was introduced. At week 26, compared to control rats, diabetic rats showed an increased A peak (790.0 ± 198.4 vs 625.9 ± 118.7 , $p < 0.05$) and A' peak (64.8 ± 9.3 vs 50.6 ± 11.1 , $p < 0.01$) and a decreased E' peak (40.1 ± 8.2 vs 65.9 ± 18.8 , $p < 0.01$), while the E peak generally remained unchanged. Accordingly, the E/A and E'/A' ratios were significantly lower in diabetic rats (1.0 ± 0.2 vs 1.4 ± 0.2 , 0.6 ± 0.1 vs 1.3 ± 0.3 , both $p < 0.01$, **Figure 1F** and **G**), and the E/E' ratio was increased in diabetic rats (20.6 ± 5.1 vs 13.9 ± 4.7 , $p < 0.01$, **Figure 1H**). Other parameters, including left ventricular end-diastolic diameter (LVEDD), left ventricular posterior wall end-diastolic thickness, and ejection fraction, were not different between the diabetic and control rats. Cardiac catheterization demonstrated that diabetic rats had a significantly lower dp/dt (7597 ± 2315.2 vs 2086.7 ± 731.7 , $p < 0.01$, **Figure 1J**) and a higher but not significantly different LVEDP than control rats (**Figure 1K**).

Histologic staining

The hearts of diabetic rats were obviously heavier than those of nondiabetic rats, while their body weight was significantly lower; thus, the heart weight to body weight ratio (HW/BW) was increased in diabetic rats ($p < 0.01$, **Figure 2**). HE staining showed that the diabetic heart was dilated, and WGA staining showed that the cross-sectional

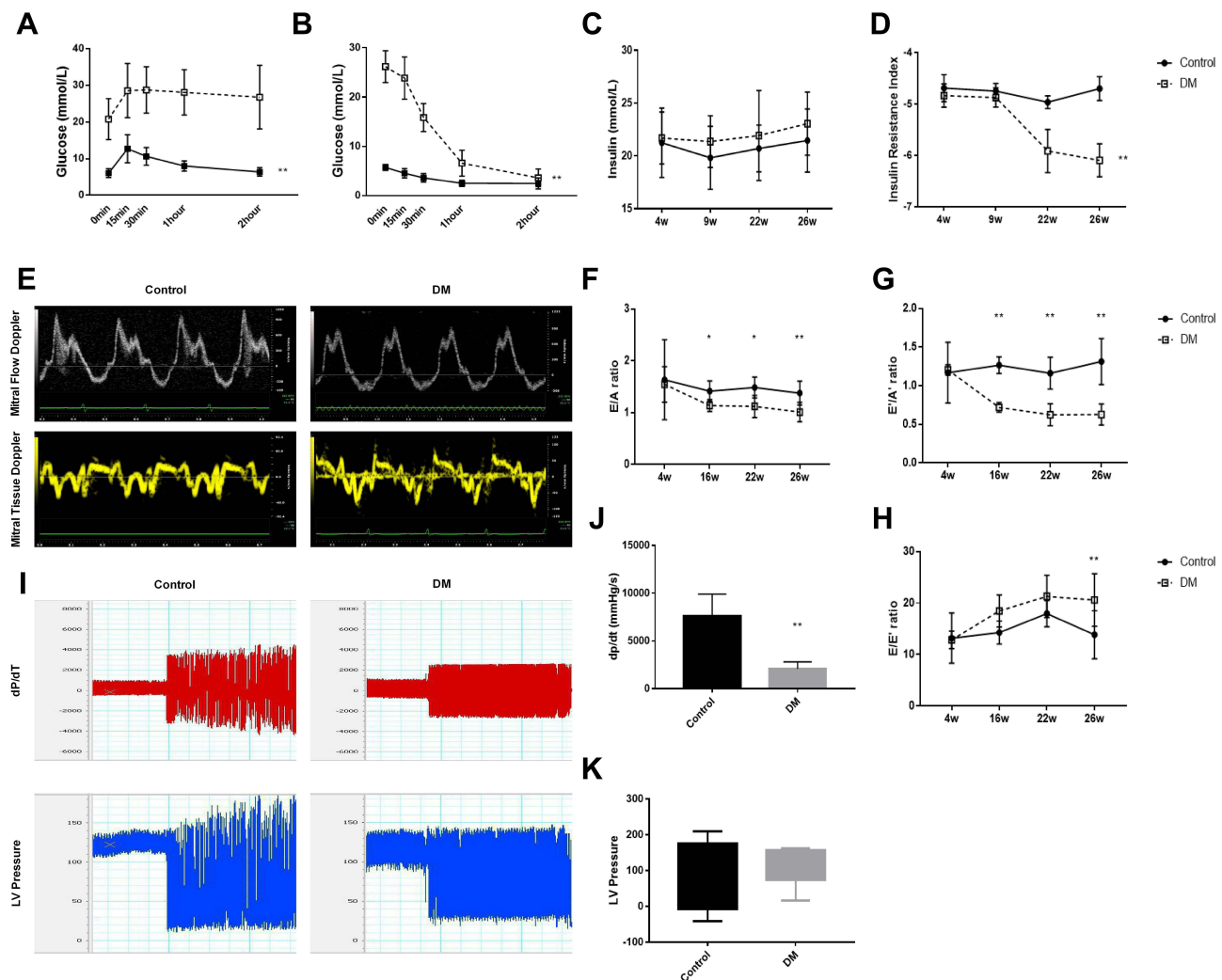


Figure 1 Glucose, insulin, echocardiography and left ventricular catheterization findings in control and DM hearts. (**A–D**): IPGTT, IPITT, fasting serum insulin, and insulin resistance index results in control and DM rats at each time point. Data are shown as *t*-test results for the AUC of the glucose curve for 8 rats in each group. (**E**): Representative images of mitral flow Doppler and tissue Doppler in control and DM rats at 26 w. (**F–H**): E/A, E'/A', and E/E' ratio in control and DM rats at each time point. Data are shown as *t*-test results for 8 rats in each group. (**I–K**): dp/dt and LVEDP in control and DM rats at 26 w. Data are shown as *t*-test results for 3 rats in each group. * $p < 0.05$ vs control; ** $p < 0.01$ vs control.

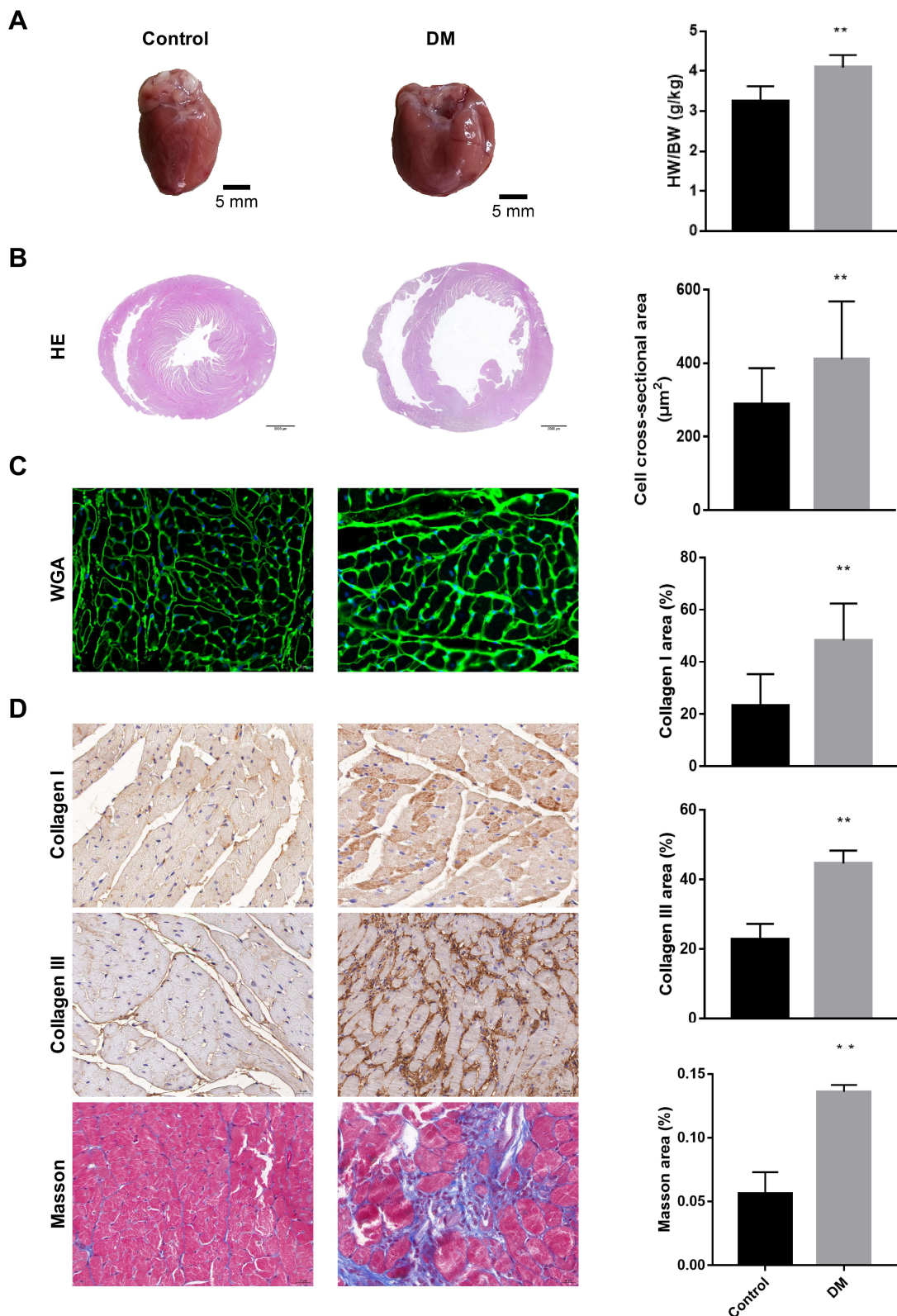


Figure 2 Cardiac fibrosis in control and DM hearts. **(A)**: General view of control and DM hearts; **(B and C)**: HE and WGA staining in control and DM hearts. The cell cross-sectional area in 8 rats in each group was compared using t tests. **(D)**: Collagen I and collagen III immunohistochemistry and Masson staining of control and DM hearts; the data for 8 rats in each group were compared using t tests. ** $p < 0.01$ vs control.

cardiomyocyte area was significantly larger in diabetic rats than in control rats ($p < 0.01$, Figure 2C). Masson staining and collagen I and collagen III immunohistochemistry demonstrated that fibrosis deposition was greatly increased in the diabetic rat hearts ($p < 0.01$, Figure 2D).

Diabetic Hearts Had Decreased STAMP2 Expression

Western blotting showed that STAMP2 expression was significantly decreased in diabetic hearts compared to control hearts ($p = 0.02$, control vs DM). After transfection with recombinant STAMP2-expressing AAV9, STAMP2 was successfully overexpressed in the recombinant STAMP2-expressing group ($p < 0.01$ vs vehicle group; $p < 0.01$ vs DM group, Figure 3).

STAMP2 Improved Glucose Tolerance and Insulin Sensitivity

Before STAMP2 was overexpressed (22 w), GTTs and ITTs showed that the AUC of the glucose curve was not significantly different among the DM, vehicle and STAMP2 groups. Four weeks after transfection (26 w), the glucose curve of the STAMP2 group diverged from that of the DM and vehicle groups in both the GTT and ITT, and the AUC was correspondingly lower than that in the DM group ($p < 0.01$ for GTT) and vehicle group ($p < 0.01$ for GTT and $p < 0.05$ for ITT, Figure 4). Fasting blood samples for serum insulin determination were taken simultaneously, and insulin was not different among the DM, vehicle and STAMP2 groups, while the ISI was increased after STAMP2 was overexpressed in the STAMP2 group. ($p < 0.05$ vs vehicle, $p < 0.01$ vs DM, Figure 4). Proteins related to insulin signaling were also investigated via Western blotting. In the DM and vehicle groups, the p-Akt/Akt ratio was greatly decreased, and IRS-1 was correspondingly decreased. STAMP2 transfection remarkably improved the p-Akt/Akt ratio and the IRS-1 level in diabetic hearts (both $p < 0.05$, vs vehicle group and DM group, Figure 4).

STAMP2 Alleviated Myocardial Fibrosis in Diabetic Hearts

As indicated above, diabetic rats had an increased HW/BW ratio and cardiac interstitial fibrosis deposition. Overexpression of STAMP2 alleviated these changes: the HW/BW ratio in the STAMP group was lower than that in the DM and vehicle groups. The STAMP2 group also had a smaller cross-sectional cellular area, less fibrosis accumulation and reduced collagen I and III deposition, as indicated by WGA, Masson and immunohistochemical staining, respectively (all $p < 0.01$, Figure 5).

STAMP2 Attenuates Diabetes-Induced Diastolic Dysfunction

As shown above, echocardiography revealed overt diastolic dysfunction before STAMP2 was overexpressed (22 w), as demonstrated by the E/A, E'/A' and E/E' ratios (Figure 6A). Four weeks after transfection (26 w), the E/A ratio was significantly elevated in the STAMP2 group compared to the DM (1.3 ± 0.12 vs 0.99 ± 0.19 , $p < 0.05$, Figure 6B) and vehicle groups (1.3 ± 0.1 vs 1.03 ± 0.2 , $p < 0.05$, Figure 6B); E'/A' was significantly elevated in the STAMP2 group compared to the DM (1.17 ± 0.14 vs 0.57 ± 0.19 , $p < 0.01$, Figure 6B) and vehicle groups (1.3 ± 0.1 vs 0.09 ± 1.17 , $p < 0.01$, Figure 6B); and E/E' in the STAMP2 group was significantly lower than in the DM (14.47 ± 4.14 vs 21.59 ± 6.55 , $p < 0.05$, Figure 6B) and vehicle groups (14.47 ± 4.14 vs 19.97 ± 4.46 , $p = 0.05$, Figure 6B). Left ventricular end-diastolic diameter (LVEDD), left ventricular posterior wall end-diastolic thickness, and ejection fraction remained unchanged among the 4 groups. Left ventricular

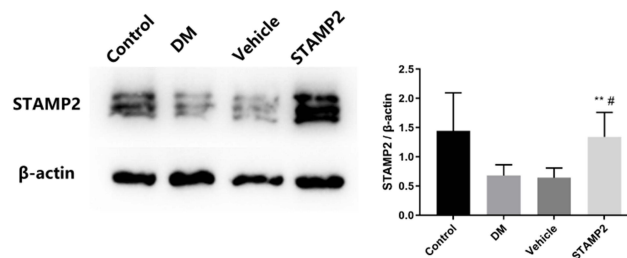


Figure 3 Representative Western blot and Western blot analysis of STAMP2 expression in the control, DM, vehicle and STAMP2 groups. Data for 6 rats in each group were compared using t tests. ** $p < 0.01$ vs vehicle; # $p < 0.05$ vs DM.

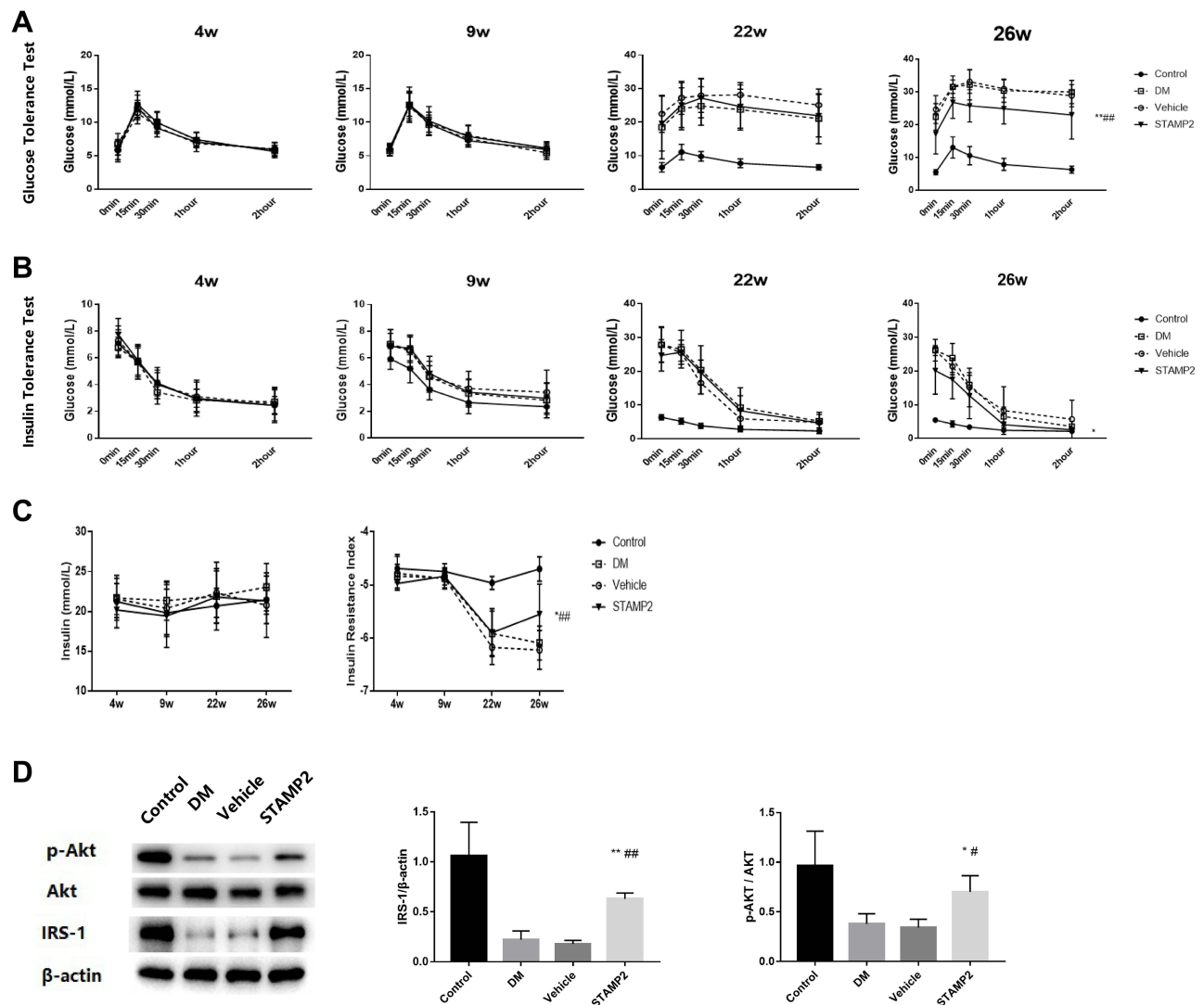


Figure 4 STAMP2 improved glucose tolerance and insulin sensitivity. **(A–B)**: IPGTTs and IPITTs in rats from the control, DM, vehicle and STAMP2 groups at each time point. Data are shown as *t*-test results for the AUC of the glucose curve for 8 rats in each group. **(C)**: Fasting serum insulin and insulin resistance index values in rats from the control, DM, vehicle and STAMP2 groups at each time point. Data for 8 rats in each group were compared using *t* tests. **(D)**: Representative Western blot and Western blot analysis of Akt, p-Akt and IRS-1 expression in the control, DM, vehicle and STAMP2 groups. Data for 6 rats in each group were compared using *t*-tests. **p*<0.05 vs vehicle, ***p*<0.01 vs vehicle, #*p*<0.05 vs DM, ###*p*<0.01 vs DM.

catheterization showed that the STAMP2 group had a higher dp/dt ratio (vs DM: 8174.13 ± 1266.37 vs 1779.74 ± 697.95 , *p*<0.01; vs vehicle: 8174.13 ± 1266.37 vs 2198.14 ± 513.23 , *p*<0.01, **Figure 6B**) and lower end-diastolic pressure than the DM and vehicle groups (vs DM: -7.1 ± 1.92 vs 43.14 ± 12.21 , *p*<0.01; vs vehicle: -7.1 ± 1.92 vs 10.97 ± 3.55 , *p*<0.01, **Figure 6B**).

STAMP2 Induces NMRAL1 Translocation to the Nucleus and Negatively Regulates NF- κ B Signaling

STAMP2 is at the intersection of the metabolic and inflammatory pathways. Thus, we examined which inflammatory signaling pathways were altered, and we found increased phosphorylation of p65 in the DM and vehicle groups, whereas phosphorylation of p65 was decreased to a significantly lower extent in STAMP2-overexpressing diabetic hearts (**Figure 7A**).

Next, we investigated how NF- κ B signaling was affected by STAMP2. As indicated above, we investigated the NMRAL1 intracellular distribution in all 4 groups via immunofluorescence staining with an anti-NMRAL1 antibody. The ratio of the nucleus with NMRAL1 embedded inside to the total nucleus (with and without NMRAL1 embedded inside) is shown. The results indicated that the ratio in the control and STAMP2 groups was significantly higher than that in the DM and vehicle groups (STAMP2 vs vehicle: $\chi^2=15.39$, *p*<0.01, STAMP2 vs DM: $\chi^2=5.40$, *p*<0.05, **Figure 7B**).

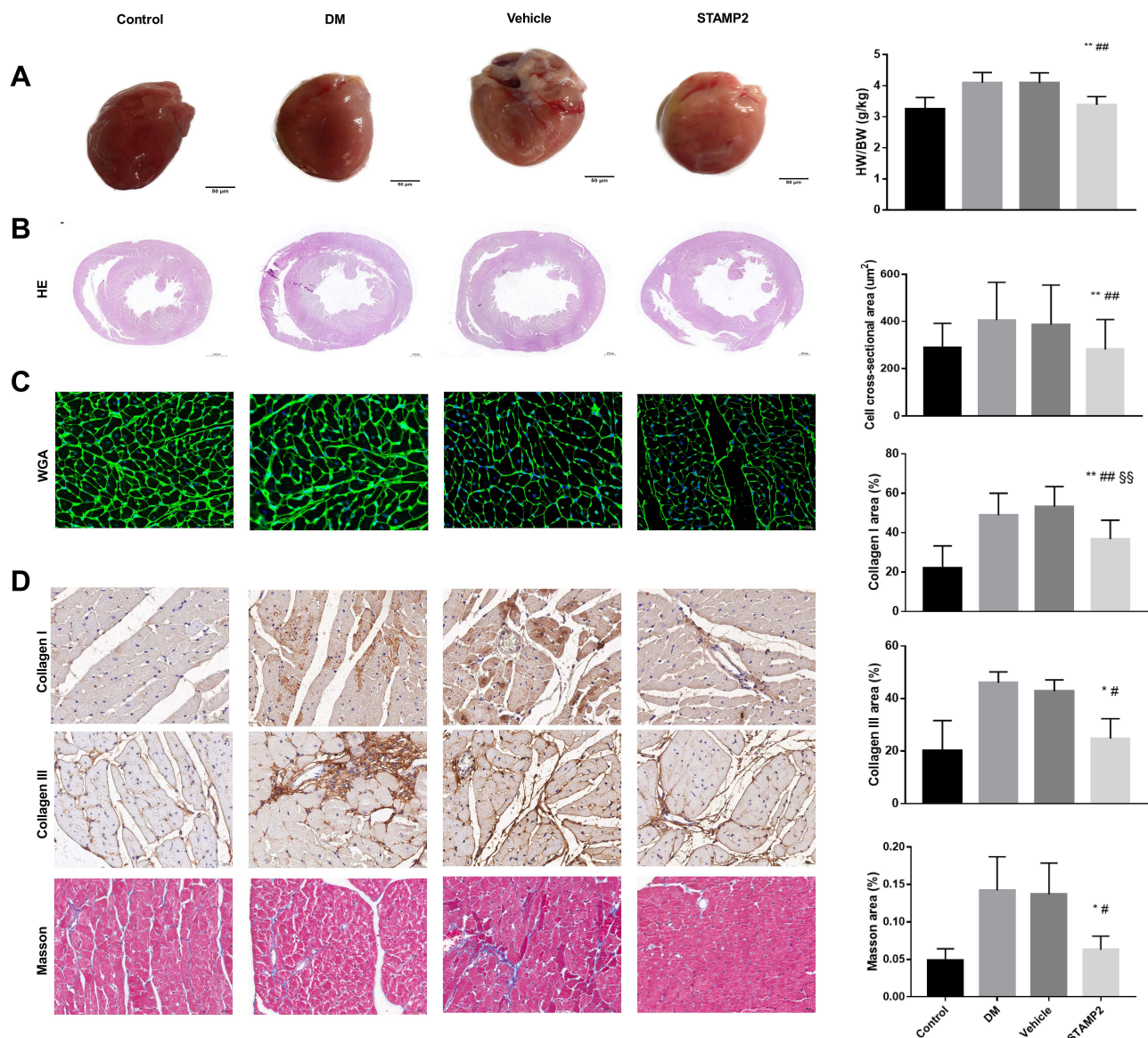


Figure 5 STAMP2 alleviated myocardial fibrosis in diabetic hearts. **(A)**: General view of rat hearts from the control, DM, vehicle and STAMP2 groups; **(B and C)**: HE and WGA staining of control, DM, vehicle and STAMP2 group hearts. The cell cross-sectional area in 8 rats from each group was compared using t tests. **(D)**: Collagen I and collagen III immunohistochemistry and Masson staining in hearts from rats in the control, DM, vehicle and STAMP2 groups. Data for 8 rats in each group were compared using t tests. * $p < 0.05$ vs vehicle, ** $p < 0.01$ vs vehicle, # $p < 0.05$ vs DM, ## $p < 0.01$ vs DM, \$\$\$ $p < 0.01$ vs control.

Discussion

According to a previous epidemiological study, the prevalence of heart failure in diabetic patients is 2 times higher than that in nondiabetic patients,¹¹ and heart failure has become the most common cardiovascular complication of diabetes mellitus.¹² Since the incidence of myocardial infarction in diabetic patients has substantially dropped during the last two decades,¹³ DCM is emerging as the main cause of heart failure in diabetic patients.² To date, no evidence has indicated that risk factor intervention can reduce the incidence and hospitalization rate of heart failure in diabetic patients.¹⁴ Antidiabetic agents have also failed, and some even make the condition worse.¹⁵ This frustrating situation urges further exploration of the deep-seated pathophysiology of DCM and new therapeutic targets for DCM.

The two major pathophysiological bases of DCM are diastolic dysfunction and extracellular matrix remodeling, which are triggered and exacerbated by insulin resistance.¹⁶ The normal and unstressed myocardium predominantly metabolizes free fatty acids (FFAs) for ATP production. However, in a stressed state (eg, ischemia, pressure load, injury), the heart

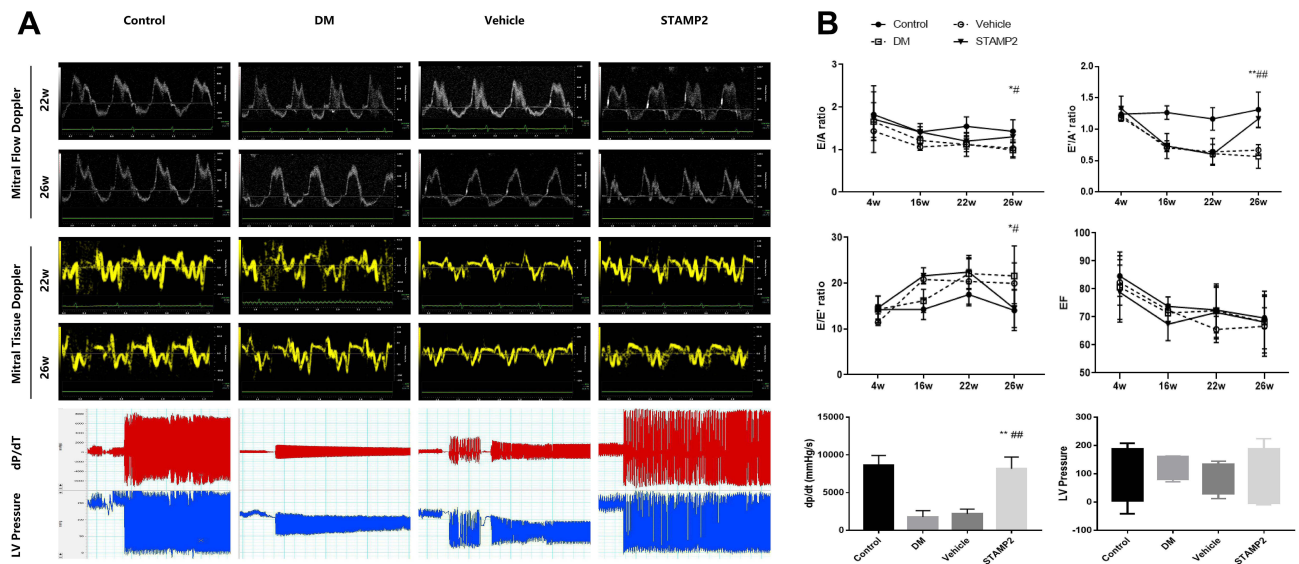


Figure 6 STAMP2 attenuates diabetes-induced diastolic dysfunction. (A): Representative mitral flow Doppler, tissue Doppler, dP/dT and LV pressure results for rats in the control, DM, vehicle and STAMP2 groups; 6 samples from each group were used for the study. (B): Analysis of the E/A, E'/A', and E/E' ratios; EF; dp/dt; and LVEDP in control, DM, vehicle and STAMP2 rats. The data are shown as t-test results for each group. *p<0.05 vs vehicle, **p<0.01 vs vehicle, #p<0.05 vs DM, ###p<0.01 vs DM.

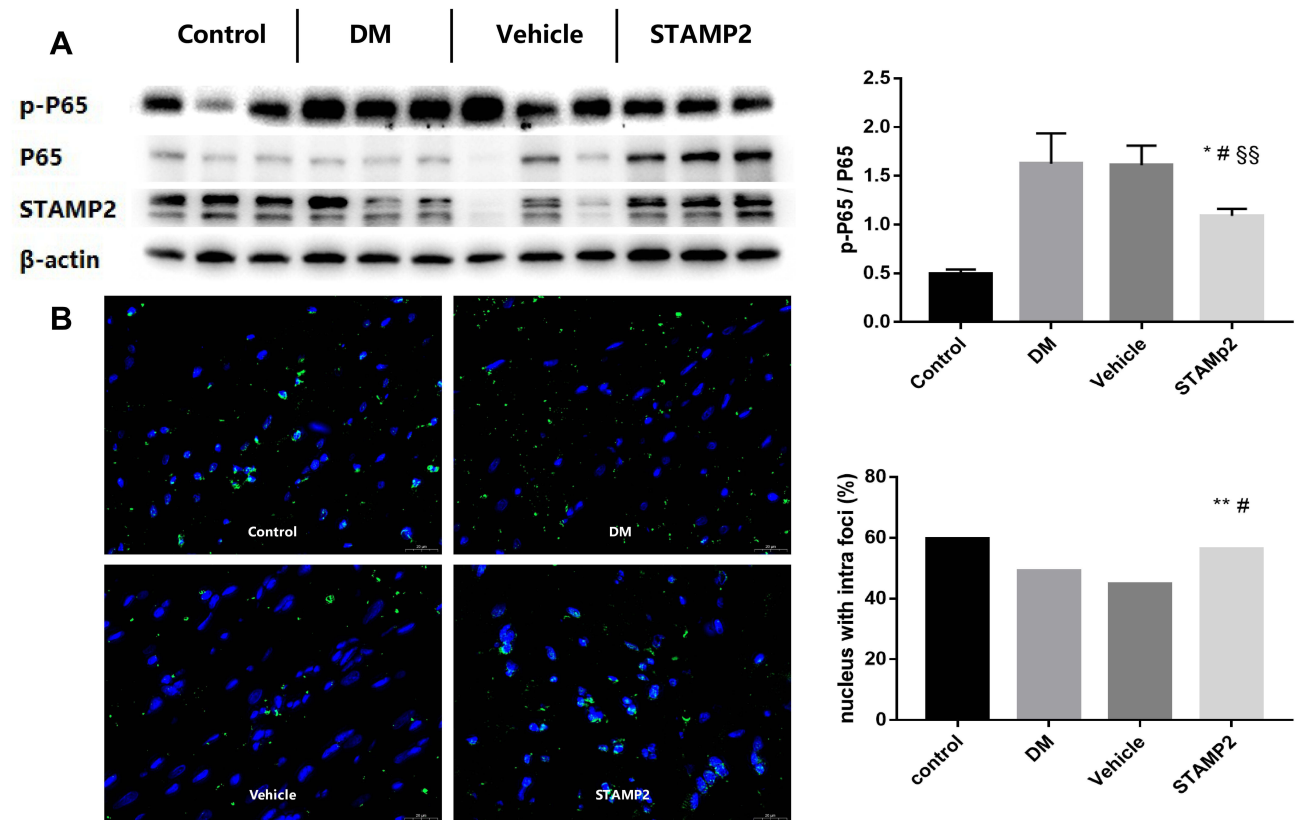


Figure 7 STAMP2 induces NMRAL1 translocation to the nucleus and negatively regulates NF-κB signaling. (A): Western blot analysis of p-p65, p65 and STAMP2 expression in the control, DM, vehicle and STAMP2 groups. Data for 6 rats in each group were compared using t tests. (B): Representative immunofluorescence of NMRAL1 showing the intra- and extranuclear distribution and ratio of nuclei with NMRAL1 imbedded to total nuclei in the control, DM, vehicle and STAMP2 groups. Data for 8 rats in each group were compared using χ^2 -tests. *p<0.05 vs vehicle, **p<0.01 vs vehicle, #p<0.05 vs DM, \$\$p<0.01 vs control.

turns to glucose as the main source of energy.¹⁷ Insulin resistance prevents this adaptive metabolic pattern switch. As a result, myocardial glucose uptake and utilization are crippled, and FFA metabolism is increased. This inappropriate reliance on FFA metabolism leads to increased oxygen consumption, decreased cardiac energy efficiency, and potentially lipotoxicity. In addition, accumulated FFA metabolic products are associated with increased reactive oxygen species (ROS) and inflammatory cytokine levels,¹⁸ which further aggravate insulin resistance.

Previous studies have found that STAMP2 alleviates insulin resistance in several metabolic disorder models, including in adipose tissue, atherosclerotic plaques, and fatty liver.^{5,19,20} Here, we found the protective role of STAMP2 in the diabetic heart is consistent with that in other metabolic organs. In the present study, we built a DCM model with classic manifestations of cardiac insulin resistance and interstitial fibrosis. After STAMP2 was specifically overexpressed in the heart via transfection with recombinant AAV9, alleviated cardiac insulin resistance and activated insulin signaling were observed. Cardiac fibrosis was also attenuated, as indicated by multiple histochemical and immunohistochemical assays. Echocardiography and left ventricular catheterization revealed that diastolic dysfunction was greatly ameliorated. All these results support the idea that STAMP2 can significantly improve cardiac fibrosis and diastolic dysfunction in diabetic hearts. Our research may identify a new promising therapy for DCM.

In addition, we investigated how STAMP2 alleviates insulin resistance. Previous studies have indicated that STAMP2 is capable of suppressing several inflammatory signaling pathways, thus improving insulin resistance.^{19,21} However, how STAMP2 restrains these inflammatory signaling pathways is still unknown. In these previous studies, Akt signaling was consistently found to be activated when STAMP2 was overexpressed. Conversely, Akt can cross-talk with several inflammatory signaling pathways, such as mTOR and NF- κ B, and promote inflammation,²² which apparently was not the reason why STAMP2 attenuated the inflammatory response. We started from the biological structure of STAMP2, as previously sequenced.²³ STAMP2 was named after the distinctive six transmembrane domains in the C-terminus and the three functional domains in the N-terminus: a dinucleotide-binding domain, an NADPH oxidoreductase motif, and a pyrroline 5-carboxylate reductase motif. In the present study, we demonstrated that the NADPH oxidoreductase motif is the key to the anti-inflammatory and anti-insulin resistance capacity of STAMP2. Nevertheless, “NMRAL1-Mediated NF- κ B Inhibition” might not be the only biological effect of the NADPH oxidoreductase motif of STAMP2. Previous research has also revealed that STAMP2 is involved in tumorigenesis^{24,25} but functions as a proinflammatory oxidative stress promoter, indicating that it might have an opposite function under different circumstances. More research, including loss-of-function research, needs to be performed in the future for further confirmation.

Several limitations of our study must be mentioned. First, due to methodological problems, reliable repeatability of NADPH level detection was not obtained in the present study, but since it has been verified in previous research,²⁶ the results are still worth considering. Second, a cellular experiment was needed to confirm the protective effect of STAMP2 after a NMRAL1 or NF- κ B antagonist was used, which will be included in future studies.

In conclusion, STAMP2 is decreased in DCM. STAMP2 improves insulin resistance by promoting NMRAL1 nuclear translocation and NF- κ B inhibition and thus attenuates cardiac fibrosis and diastolic dysfunction.

Funding

This work was supported by research grants from the National Natural Science Foundation of China (82070392, 81900332, 30971215) and the Science and Technology Planning Project of Wenzhou, Wenzhou, China (Y20210135).

Disclosure

The authors declare that the research was conducted in the absence of any commercial or financial relationships that could be construed as a potential conflict of interest.

References

1. Aronow WS, Ahn C. Incidence of heart failure in 2737 older persons with and without diabetes mellitus. *Chest*. 1999;115(3):867–868. doi:10.1378/chest.115.3.867

2. Guanhong J, Hill Michael A, Sowers James R. Diabetic cardiomyopathy, an update of mechanisms contributing to this clinical entity. *Circ Res*. 2018;122(4):624–638. doi:10.1161/CIRCRESAHA.117.311586
3. Ohgami RS, Campagna DR, McDonald A, Fleming MD. The Steap proteins are metalloredoxases. *Blood*. 2006;108(4):1388–1394. doi:10.1182/blood-2006-02-003681
4. Wellen KE, Fucho R, Gregor MF, et al. Coordinated regulation of nutrient and inflammatory responses by STAMP2 is essential for metabolic homeostasis. *Cell*. 2007;129(3):537–548. doi:10.1016/j.cell.2007.02.049
5. Han L, Tang MX, Ti Y, et al. Overexpressing STAMP2 improves insulin resistance in diabetic ApoE^{-/-}/LDLR^{-/-} mice via macrophage polarization shift in adipose tissues. *PLoS One*. 2013;8(11):e78903. doi:10.1371/journal.pone.0078903
6. Kim HY, Park SY, Lee MH, et al. Hepatic STAMP2 alleviates high fat diet-induced hepatic steatosis and insulin resistance. *J Hepatol*. 2015;63(2):477–485. doi:10.1016/j.jhep.2015.01.025
7. Moldes M, Lasnier F, Gauthereau X, et al. Tumor necrosis factor- α -induced adipose-related protein (TIARP), a cell-surface protein that is highly induced by tumor necrosis factor- α and adipose conversion. *J Biol Chem*. 2001;276(36):33938–33946. doi:10.1074/jbc.M105726200
8. Lian M, Zheng X. HSCARG regulates NF- κ B activation by promoting the ubiquitination of RelA or COMMD1. *J Biol Chem*. 2009;284(27):17998–18006. doi:10.1074/jbc.M809752200
9. Zheng X, Dai X, Zhao Y, et al. Restructuring of the dinucleotide-binding fold in an NADP(H) sensor protein. *PNAS*. 2007;104(21):8809–8814. doi:10.1073/pnas.0700480104
10. Hernandez R, Zhou C. Recent advances in understanding the role of IKK β in cardiometabolic diseases. *Front Cardiovasc Med*. 2021;8:752337. doi:10.3389/fcvm.2021.752337
11. Kenny HC, Abel ED. Heart failure in type 2 diabetes mellitus. *Circ Res*. 2019;124(1):121–141. doi:10.1161/CIRCRESAHA.118.311371
12. Dinesh Shah A, Langenberg C, Rapsomaniki E, et al. Type 2 diabetes and incidence of a wide range of cardiovascular diseases: a cohort study in 1.9 million people. *Lancet*. 2015;385(Suppl 1):S86. doi:10.1016/S0140-6736(15)60401-9
13. Gregg EW, Li Y, Wang J, et al. Changes in diabetes-related complications in the United States, 1990–2010. *N Engl J Med*. 2014;370(16):1514–1523. doi:10.1056/NEJMoa1310799
14. Tate M, Grieve DJ, Ritchie RH. Are targeted therapies for diabetic cardiomyopathy on the horizon? *Clin Sci*. 2017;131(10):897–915. doi:10.1042/CS20160491
15. American Diabetes Association. Disclosures: standards of medical care in diabetes-2019. *Diabetes Care*. 2019;42(Suppl 1):S184–6. doi:10.2337/dc19-Sdis01
16. Fang ZY, Prins JB, Marwick TH. Diabetic cardiomyopathy: evidence, mechanisms, and therapeutic implications. *Endocr Rev*. 2004;25(4):543–567. doi:10.1210/er.2003-0012
17. An D, Rodrigues B. Role of changes in cardiac metabolism in development of diabetic cardiomyopathy. *Am J Physiol Heart Circ Physiol*. 2006;291(4):H1489–1506. doi:10.1152/ajpheart.00278.2006
18. Ferdinando G, Michael B, Marie SA, Schmidt AM. Oxidative stress and diabetic complications. *Circ Res*. 2010;107(9):1058–1070. doi:10.1161/CIRCRESAHA.110.223545
19. Wang F, Han L, Qin R, et al. Overexpressing STAMP2 attenuates adipose tissue angiogenesis and insulin resistance in diabetic ApoE^{-/-}/LDLR^{-/-} mouse via a PPAR γ /CD36 pathway. *J Cell Mol Med*. 2017;21(12):3298–3308. doi:10.1111/jcmm.13233
20. Wang J, Han L, Wang ZH, et al. Overexpression of STAMP2 suppresses atherosclerosis and stabilizes plaques in diabetic mice. *J Cell Mol Med*. 2014;18(4):735–748. doi:10.1111/jcmm.12222
21. Oh YJ, Kim HY, Lee MH, et al. Cilostazol Improves HFD-Induced Hepatic Steatosis by Upregulating Hepatic STAMP2 Expression through AMPK. *Mol Pharmacol*. 2018;94(6):1401–1411. doi:10.1124/mol.118.113217
22. PI3K/Akt Signaling [Internet]. Cell signaling technology; [cited August 7, 2022]. Available from: <https://www.cellsignal.com/pathways/pathways-akt-signaling>. Accessed October 12, 2022.
23. Korkmaz CG, Korkmaz KS, Kurys P, et al. Molecular cloning and characterization of STAMP2, an androgen-regulated six transmembrane protein that is overexpressed in prostate cancer. *Oncogene*. 2005;24(31):4934–4945. doi:10.1038/sj.onc.1208677
24. Orfanou IM, Argyros O, Papapetropoulos A, Tseleni-Balafouta S, Vougas K, Tamvakopoulos C. Discovery and pharmacological evaluation of STEAP4 as a novel target for HER2 overexpressing breast cancer. *Front Oncol*. 2021;11:608201. doi:10.3389/fonc.2021.608201
25. Jin Y, Wang L, Qu S, et al. STAMP2 increases oxidative stress and is critical for prostate cancer. *EMBO Mol Med*. 2015;7(3):315–331. doi:10.15252/emmm.201404181
26. ten Freyhaus H, Calay ES, Yalcin A, et al. Stamp2 controls macrophage inflammation through nicotinamide adenine dinucleotide phosphate homeostasis and protects against atherosclerosis. *Cell Metab*. 2012;16(1):81–89. doi:10.1016/j.cmet.2012.05.009

Diabetes, Metabolic Syndrome and Obesity: Targets and Therapy

Dovepress

Publish your work in this journal

Diabetes, Metabolic Syndrome and Obesity: Targets and Therapy is an international, peer-reviewed open-access journal committed to the rapid publication of the latest laboratory and clinical findings in the fields of diabetes, metabolic syndrome and obesity research. Original research, review, case reports, hypothesis formation, expert opinion and commentaries are all considered for publication. The manuscript management system is completely online and includes a very quick and fair peer-review system, which is all easy to use. Visit <http://www.dovepress.com/testimonials.php> to read real quotes from published authors.

Submit your manuscript here: <https://www.dovepress.com/diabetes-metabolic-syndrome-and-obesity-targets-and-therapy-journal>